Polymer Bulletin (2020) 77:2111–2137
https://doi.org/10.1007/s00289-019-02846-4

ORIGINAL PAPER

Thermal degradation of poly(lactic acid)–zeolite composites produced by melt-blending

Marçal Pires[2] · Marius Murariu[1] · Ariela M. Cardoso[2] · Leila Bonnaud[1] · Philippe Dubois[1]

Received: 18 December 2018 / Revised: 13 June 2019 / Accepted: 17 June 2019 /
Published online: 21 June 2019

Abstract

Various zeolites (4A, Y, 13X) and related fillers (molecular sieves and coal fly ash) were used to prepare PLA composites and to assess their degrading effect on the polyester matrix under different processing conditions, at various zeolite/filler loadings. In this objective, untreated fillers, as well as washed and thermally activated zeolites, were used. PLA–zeolite composites were produced by melt-blending step followed by the evaluation of rheological information and molecular and thermal characteristics. The degradation of PLA during the preparation and processing of PLA–zeolite composites, or due to the presence of fillers, was evidenced by specific analyses (SEC, DSC, TGA, TG-FTIR). PLA degradation was mainly dependent on the nature of zeolite, filler loading, and thermal and processing history. The results of the study suggest that a stronger degradation effect is obtained by the addition of zeolite 4A into PLA (at loading of 5–10%) with respect to other zeolites (e.g., 13X and Y). It was also revealed the key roles of the temperature and residence time (as parameters in melt-mixing process), free alkalinity level, and water uptake in determining the ultimate characteristics of composites. The washing and thermal activation pretreatments of fillers have diminished in some cases the degradation of PLA matrix. Finally, the study also highlights the zeolite grades capable of being used to produce new PLA composites with competitive properties and those that could be of interest to improve PLA recycling by pyrolysis.

Keywords Poly(lactic acid) (PLA) · Zeolites · Composites · Thermal degradation

Electronic supplementary material The online version of this article (https://doi.org/10.1007/s00289-019-02846-4) contains supplementary material, which is available to authorized users.

✉ Marçal Pires
mpires@pucrs.br

[1] Center of Innovation and Research in Materials and Polymers (CIRMAP), Laboratory of Polymeric and Composite Materials, University of Mons & Materia Nova Research Center, Place du Parc 20, 7000 Mons, Belgium

[2] Laboratory of Environmental Analytical Chemistry, School of Sciences, Pontifical Catholic University of Rio Grande do Sul, Porto Alegre 90619-900, Brazil

Introduction

The swift expansion in the production of biopolymers is connected to the increased demand for new environmentally sustainable products and to the higher restrictions for the use of polymers with high "carbon footprint" of petrochemical origin, particularly in packaging, automotive, electrical, and electronics industries. Recently, as one key alternative and in competition with the petroleum-based polymers, poly(lactic acid) or polylactide (PLA) was considered as one of the most promising sustainable candidates for further development. The leading position of PLA on the market of bio-based polymers is due to its relevant performances (i.e., high tensile strength and stiffness), whereas the biosourced origin and (in some cases) the properties of biodegradation can represent in specific applications an additional advantage [1–5]. The last trends and forecasts reveal also that PLA is more and more appealing, not only for conventional utilization such as packaging and textile materials, but also for engineering/technical sectors [6]. However, novel grades of PLA and PLA-based materials with improved performances and higher added value are continuously looked for various applications. Thus, on the one hand, to reach the end-user demands, the PLA properties can be tuned up by combining this biopolyester with various polymeric and non-polymeric dispersed phases: micro- and nanofillers, flame retardants, impact modifiers, plasticizers, and other additives [1, 3, 5–11]. On the other hand, following the actual industrial progress, the recyclability of PLA is one key aspect that is recently considered. The production and processing of PLA requires a considerable amount of energy; thus even compostable and biosourced polymers should be recycled as much as possible using traditional or non-conventional techniques [12].

In this context, it is noteworthy reminding that the pyrolysis of waste thermoplastics at high temperature (500–850 °C) has been investigated to produce low molecular weight hydrocarbons as fuels and other chemicals [13–16]. However, this degradation/pyrolysis process needs a great quantity of energy, and some solid catalysts have been proposed to decrease the degradation temperature and energy requirement but increasing the yield of liquid products [17]. Interestingly, some fillers such as the zeolites are widely used not only to produce material composites with specific end-use properties having as matrix various polymers (polyethylene (PE), polypropylene (PP), polystyrene (PS), PLA), but also as solid catalysts in polymer degradation studies, due to their strong acidity, specific pore size, and structure effects [18–21].

Zeolites are microporous crystalline hydrated aluminum–silicates, while over 200 synthetic and 40 naturally occurring grades are known [22]. Structurally, zeolites are aluminum-silicate-based frameworks, which are built on infinitely extending three-dimensional $[AlO_4]^{5-}$ and $[SiO_4]^{4-}$ tetrahedral linked to each other by sharing all the oxygen atoms. Zeolites are known for their remarkable thermal and chemical stability and are most commonly used in particulate form as catalysts, detergent builder, ion exchanger, and gas separation media. Personal hygiene products, such as those used for odor removal and medical applications,

represent other uses of this versatile, non-toxic, and inexpensive material. All these applications take the advantage of the uniform microporosity (and even nanoporosity) of zeolites (0.3–1.3 nm), which allows applications by the separation/sieving of molecules according to their size with precision of a fraction of nanometer. Interestingly, new zeolite applications may lie upon their addition into thermoplastic polymers for reducing odor and VOC emissions [20, 23] but also as carriers of silver particles to design functional materials assessing strong antibacterial activity, among other applications [21, 24, 25].

Still, the use of different types of zeolites as degradation agent of polyolefins is well documented in the literature [26–30]. The catalytic effect of the zeolites is attributed not only to their acid strength [27, 28] but also to other structural parameters, such as pore structure and size, which could also play a key role [29]. It is suggested a participation of inner surface of these zeolites in degradation despite the fact that the reactant molecules are extremely large [28]. The activation energy of polymer cracking over zeolite is lower compared with other commercial catalysts such as clays [30], resulting in significant decreases of the polymer pyrolysis temperature.

Regarding the production of new bio-based compounds, it is noteworthy mentioning that some studies have been concerned the preparation, characterization, and thermal degradation of PLA–zeolite composites [31–39]. However, the development of special formulations of biopolymers is clearly in its early stages compared with the utilization of conventional polymers. As it was reported in the literature, the addition of zeolites into bio-based PLA may hold promise for some specific applications such as packaging systems, e.g., films with controlled permeation selectivity to CO_2/O_2 [32]. Yuzay et al. [33] reported also the preparation of PLA (94% L-lactide)–synthetic zeolite (4A, Si/Al = 1, pore size of 38–40 nm) composites using a melt-compounding process and the effects of 4A synthetic zeolites on PLA physical–mechanical properties. PLA composites containing up to 5 wt% zeolite 4A were prepared using a microextruder (temperature of melt compounding of 185 °C), and the mini-injection molding was used to prepare the test specimens for physical and mechanical characterization. The TEM and SEM images of composites indicated neither void formation around the zeolite particles nor cavities in the PLA matrix, indicating the existence of good interfacial adhesion between zeolite and this polyester, assumption which is confirmed also by the mechanical testing. These authors also reported the preparation of PLA composites containing 5 wt% synthetic (4A, framework type LTA, Si/Al1.0) and natural (chabazite, CHA, Si/Al 2.4–3.4) zeolites using the extrusion/injection molding techniques [33]. DSC results revealed that the glass transition and melting temperatures were not significantly changed. However, the incorporation of both 4A and chabazite zeolites enhanced the nucleation of PLA crystallites as well as increased the percent crystallinity. TGA results showed that at temperatures above 300 °C, PLA–zeolite 4A composites were thermally decomposed more easily than the PLA and PLA–chabazite composites.

Gregorova et al. [39] studied viscoelastic properties of mineral-filled PLA composites (produced by solvent casting) using DMA and SEM techniques. The authors filled PLA with 20 wt% of three minerals: mica, natural zeolite (type not informed), and vansil, with same size (5 μm) but differing in the particle shape and surface area.

Both damping reduction and SEM analysis revealed that zeolite was better distributed in the PLA matrix than other fillers. The interfacial filler/matrix adhesion proved to be the key factors determining thermal and mechanical properties of reinforced composite material. Bendahou et al. [35] prepared PLA composites using two zeolites (type not informed) with micro- and nanosizes doped with copper and PEG as stabilizer, by melt-mixing process for packaging applications. The two fillers presented similar barrier and antibacterial properties for loading up to 12 wt%. However, better mechanical and physical properties were observed for nanosize zeolite, ensured only when a PEG (M_w 1000 g/mol) is used for the surface coating of filler.

Ye et al. [34] reported the thermal features and decomposition kinetics of PLA filled with β-zeolite (BEA, Si/Al 38) using TG/DTG analyses at different heating rates. The thermal degradation of PLA/β-zeolite composites, produced by solvent casting, is observed to mainly occur in the temperature range of 550–675 K, with β-zeolite decreasing the thermal decomposition temperature of PLA.

Hao et al. [37] performed TG/DTA analysis on PLA filled with ZSM-5 zeolite (MFI, Si/Al 25) at two loadings (10 and 20 wt%) [37, 38] and zeolite Hβ (BEA, Si/Al) [38], prepared by solvent casting. While zeolite Hβ has rendered PLA less thermally stable, the incorporation of ZSM-5 zeolite has substantially boosted the thermal degradation temperature of PLA. However, this enhancement tends to drop down when more ZSM-5 zeolite is used (from 10 to 20 wt%). Hao and Zhuang [38] concluded that the effect of zeolite on thermal degradation of PLA is much more complicated than expected, and further study is required to understand these thermal decomposition features.

However, despite the fact that some investigations are dealing with the thermal degradation of PLA induced by zeolites, studies regarding the uses of these fillers for improving the feedstock recyclability and/or degradation of PLA were not yet systematically addressed.

The aim of this study is to assess the effects of several zeolites and related fillers (molecular sieves and coal fly ash) on the depolymerization of PLA composites during their preparation and processing and in thermal evaluations using specific laboratory techniques. For this objective, detailed characterizations of the untreated fillers, as well as of the washed and thermally activated zeolites, are done. In the perspective of extrapolation at a larger scale, PLA–zeolite composites are obtained by melt blending (as one key technique used in industry), and then, the evaluation of molecular, rheological, and thermal parameters is performed and discussed. Furthermore, the comparative characterization has been realized to highlight the zeolite grades able to produce by melt-blending (MB) composites with competitive properties (molecular, thermal, etc.) or to induce the degradation of the biopolyester matrix in the perspective of PLA recycling trough a catalytic depolymerization process.

Experimental

Materials, reagents, and zeolite treatments

Poly(lactic acid), hereafter called PLA, supplier NatureWorks LLC, was a grade designed for the extrusion of films (4032D) with $M_n = 133{,}000$; dispersity (D, $M_w/M_n = 1.94$, M_w and M_n, being respectively, the weight- and number-average molar mass expressed in polystyrene equivalent). According to the producer, the other characteristics are as follows: D isomer content = 1.4%; relative viscosity = 3.94; residual monomer = 0.14%.

Several particles were used to prepare PLA composites including commercial grades of zeolites Y (Merck), 4A and 13X (IQE, Spain), and molecular sieves (m.s.) Ag-exchanged (Sigma, 35% Ag), 3A and 5A (Merck), as well as synthesized zeolite 4A (namely $4A_{PUC}$ [40]). Molecular sieves (m.s.) Ag-exchanged, 3A and 5A pellets (6–8 mesh), were ground in a mortar with a pestle and sieved (< 250 μm) and are referred as 13X-Ag m.s., 3A m.s., and 5A m.s., respectively. Coal fly ash (CFA) powder sample, from Brazilian coal combustion plant [41], was also used in some tests because its composition is similar to zeolites (aluminosilicates). It is interesting to note that CFA was used a raw material in the synthesis of zeolite $4A_{PUC}$ and was reported in the scientific literature by Cardoso et al. [40]. Table 1 gathers the main characteristics (structures, chemical formulae, pore diameter, etc.) of the zeolites and molecular sieves used in this work.

Before use, the samples of selected zeolites were pretreated by washing and heat activation. The washing process (10 g zeolite/250 mL deionized water, stirring by 800 rpm during 90 min at the temperature of 70 °C) was performed to remove the free alkalinity. The washed zeolites are indicated by the suffix "clean." The heat activation (stepwise, thermal treatment in a Nabertherm 3L furnace at 350–420 °C, 2 h, under air) aimed to eliminate water molecules and any other volatile contaminants present on and inside of zeolites. The "activated" fillers obtained after this process are indicated by the suffix "act."

Pellets of NaOH (Merck) were ground in a mortar and sieved (< 250 μm) and then added to the fly ash in the ratio of 1:10. The mixture was homogenized, dried (105 °C for 2 h), and named CFA_{NaOH}. The sodium hydroxide was added to fly ash to simulate the free alkalinity of zeolites.

Composites preparation

In this work, PLA–zeolite composites were prepared by melt blending (MB). PLA was dried in a vacuum oven (at the temperature of 60 °C for 4 h), whereas the fillers were dried at 105 °C for 2 h, before the preparation of composites. In MB procedure, zeolite fillers and other reactants were added together with PLA pellets at processing temperature (T_{MB}) of 190 °C under moderate mixing by using a Brabender bench scale kneader (cam blades). The following specific procedure was used: 2 min of premixing at 30 rpm speed to avoid an excessive increase in the torque during

Table 1 Identification and main characteristics of the zeolites and molecular sieves used in the frame of experimental program

Filler	Code	Structure type*	Cationic form	Nominal pore diameter (Å)	Si/Al	Residual alkalinity Na_2O (%)	Hydrated zeolite formulae	Binder	Form
Zeolites									
	4A**	LTA	Na	3.9	1.0	0.43	$Na_2Al_2Si_2O_8 \times 4.5\ H_2O$	None	Powder
	13X	FAU	Na	8	1.2	0.16	$Na_2O{\cdot}Al_2O_3{\cdot}2{,}5SiO_2{\cdot}6H_2O$	None	Powder
	Y	FAU	Na	8	2.4	0.07	$NaAlSi_{2,43}O_{6,86} \times 4.46H_2O$	None	Powder
Molecular sieves									
	3A m.s.	LTA	K, other	3	1.0	0.17	$K_2Al_2Si_2O_8 \times 4.5\ H_2O$	Clays	Pellets
	5A m.s.	LTA	Ca, others	4.3	1.0	0.14	$CaAl_2Si_2O_8 \times 4.5H_2O$	Clays	Pellets
	13X-Ag m.s.	FAU	Na, Ag, others	n.i.	n.i.	0.05	(Ag 35 wt%)	Clays	Pellets

*Zeolitesframework types FAU—Faujasite and LTA—Linde type A [22], **Synthetized 4A zeolite ($4A_{PUC}$) present similar characteristics; n.i. not informed

melting of PLA, followed by 5 min of mixing at 60 rpm. For comparison, pristine PLA was processed under similar conditions of melt compounding. Plates and films for different characterizations were produced by compression molding at 190 °C by using an Agila PE20 hydraulic press (program detailed in Supplementary Material, Table S1).

In the case of PLA–zeolite 4A composites, a second MB experiment was performed with sampling of low quantity of composite (< 0.5 g) during the processing at residence time of 3, 5, and 7 min. Half of the subsamples were processed by compression molding, following the same procedure indicated previously, and both parts were stored in plastic bags for analysis.

Throughout this contribution, all percentages are given as weight percent (wt%). All specimens were kept in a laboratory room with controlled temperature and humidity prior further characterization and testing. The different types of compositions elaborated in the frame of this work are gathered in Table 2.

Characterization

Thermogravimetric analyses (TGA) were performed with TGA Q5000 (TA Instruments) and using a heating ramp of 20 °C min^{-1} under airflow, from room temperature up to 800 °C (platinum pan, 60 cm^3 min^{-1} airflow rate). The decomposition temperature (T_D from DTG) and the corresponding temperatures where the samples lost 5% and 50% of their weight were obtained in accordance with ASTM E1131-03. $T_{5\%}$ was considered as the initial decomposition temperature/the onset of thermal degradation. The total water content in the samples was estimated from the TGA data and expressed on a wet basis (as received).

Differential scanning calorimetry (DSC) measurements were performed with DSC Q2000 (TA Instruments) under nitrogen flow. Samples of 7–10 mg were non-hermetically sealed in an aluminum pan and heated from room temperature to 200 °C, cooled to 0 °C, and heated again to 200 °C, all at 10 °C min^{-1}. A heat–cool–heat cycle was used to evidence the thermal events. Characteristic glass transition (T_g), cold crystallization (T_c), and melting (T_m) temperatures are reported from the second heating run. Crystallinity (χ_c) was calculated using the following equation:

$$\chi_c = \frac{\left(\Delta H_m - \Delta H_c\right)}{\Delta H_f^{100\%}} \times \frac{100}{1 - w} \quad (1)$$

where ΔH_m is the enthalpy of melting, ΔH_c is the enthalpy of cold crystallization, $\Delta H_f^{100\%}$ is the enthalpy of fusion of 100% crystalline PLA (93 J g^{-1}) [42, 43], and w is the weight fraction of zeolite in the composite [33]. Three specimens were tested for each composite.

Thermal analysis coupled with Fourier transform infrared spectroscopy (TG-FTIR) was carried out at a heating rate of 10 °C min^{-1} (from ambient temperature up to 600 °C) on a TG 209 instrument (NETZSCH, Germany) which was connected to Tensor 27 FTIR (Bruker, Germany) through stainless steel tubing. Dry nitrogen

Table 2 Identification of PLA–zeolite composites (produced by melt-blending at 190 °C) and thermal analyses and results of molecular and thermal analyses characterization

Composition		Molecular parameter		DSC							TGA			
Zeolite/m.s. Type	Loading wt%	M_n Da	D	T_g °C	T_c °C	T_m		ΔH_c J g^{-1}	ΔH_m J g^{-1}	χ_c %	$T_{5\%}$ °C	$T_{50\%}$ °C	T_D °C	Residue %
						T_{m1} °C	T_{m2} °C							
Neat PLA	0.0	109,700	2.0	62	112	162	168	30	33	3	342	378	386	0.0
4A	2.5	41,000	1.9	60	109	159	166	34	41	8	293	345	357	2.0
	5.0	13,300	2.0	56	100		161	33	42	12	269	328	341	5.0
	7.5	9,700	2.4	53	97		157	36	41	10	262	329	345	6.5
	10.0	11,300	1.8	42	97		157	33	38	6	249	326	338	8.5
Cleaned	5.0	38,800	2.1	58	101		164	29	41	13	279	340	356	5.0
Activated	5.0	23,900	2.1	60	110	155	163	36	38	2	277	338	342	4.8
$4A_{PUC}$	5.0	8,500	2.7	62	109	160	167	30	36	6	288	354	367	4.5
13X	2.5	101,700	1.9	60	107	158	165	35	42	7	354	382	386	2.0
	5.0	89,900	1.9	61	111	161	168	31	36	6	354	382	382	5.0
	10.0	58,700	2.0	61	100	163	168	30	42	46	337	385	389	8.9
Cleaned	5.0	98,500	2.2	62	115	163	168	32	35	3	344	373	377	4.0
Activated	5.0	118,100	1.9	61	108	160	167	30	35	5	347	376	379	4.0
Y	5.0	68,100	2.2	61	113	162	168	32	42	11	319	352	354	3.9
Activated	5.0	102,700	2.2	65	114		171	6	13	8	317	350	353	5.1
13X-Ag m.s.	3.0	101,000	2	62	114	164	170	29	33	4	334	366	368	3.0
	6.0	102,300	1.9	63	113	163	170	27	31	5	336	367	370	4.0
	9.0	74,200	2.4	62	113	163	170	27	33	6	327	365	366	8.0
3A m.s.	5.0	72,900	2.1	61	101		167	25	38	14	293	345	354	5.0
5A m.s.	5.0	86,300	2.2	61	101		167	23	40	19	339	379	386	2.0

gas with a flow of 60 mL min^{-1} carried the decomposition products through steel tubing into the gas cell for IR detection. Both the transfer line and the gas cell were kept at 250 °C to prevent gas condensation. IR spectra were recorded in the spectral range of 4000–650 cm^{-1} with a 4 cm^{-1} resolution and averaging 8 scans.

X-ray diffraction (XRD) analysis was used for fillers identification using a Phillips PW 1830/PW 1050 apparatus with CuK at 2θ angle between 5° and 40°.

Size exclusion chromatography (SEC) was used to determine the molecular parameters: number and weight-average molar mass expressed in polystyrene equivalent ($M_{n(PS)}$ and $M_{w(PS)}$, respectively), and the dispersity index ($D = M_w/M_n$) of pristine PLA and PLA separated from PLA–zeolite composites. Subsamples were dissolved in chloroform (8 mg polymer/4 mL solvent) and filtrated (PTFE membrane, 0.22 µm). This analysis was realized with a chromatograph equipped with a Waters 1515 isocratic pump, a Waters 717 autosampler, a series of Waters Styragel columns (HR4, HR3 and HR2), and a Waters 2414 refractive index detector interface with Water Breeze software (Waters Inc., Milford, MA, USA).

Scanning electron microscope (SEM) equipped with secondary electron and backscattered electron detectors (FEI Quanta 200FEG) was used to investigate zeolites morphology and their distribution in the polymer matrix. Chemical analysis was performed using a coupled energy-dispersive X-ray spectroscopy (EDX) analyzer.

Free alkalinity of zeolites was determined in the extracts obtained in the washing process, by acid titration (0.1 M HCl), and the values were expressed as free Na_2O (%, wt). Granulometric size distributions of fillers were carried out with a laser diffraction particle size analyzer Mastersizer 3000 (Malvern Instruments Ltd) using water as the medium of dispersion. Vapor water uptake static tests were performed on the activated powder zeolites in a controlled atmosphere system (20 ± 2 °C, relative humidity 85 ± 3%), measuring the mass gain of the samples at different time intervals (from 2 min up to 48 h), and results are expressed on dry basis.

Results and discussion

Fillers characterization and zeolite water uptake as source of PLA degradation

Figure S1 (Supplementary Material) presents the morphology and chemical composition as determined by SEM–EDX and granulometric size distribution of the zeolites (4A, $4A_{PUC}$, 13X and Y), molecular sieves (3A m.s., 5A m.s, 13X-Ag m.s), and coal fly ash (CFA) used in this study. Typical crystal morphology of 4A (cube shape),13X (polyhedron shape), and Y (octahedral shape) zeolites and fly ash (cenospheres) were observed [44, 45]. On the other hand, m.s. presents less clear morphology with clusters of smaller particles of different shapes, probably clays (< 2 µm). Zeolites 3A and 5A are obtained by ion exchange of zeolite 4A, with compensation cations K^+, Ca^{2+}, and Na^+, respectively, and present very similar cubic shape [46]. However, the m.s. fabrication process (grinding, calcination, and extrusion) probably modified typical zeolite A structures. For all the fillers, most of the particles are in the range of 1–10 µm with larger average diameters for m.s.

(7–32 µm) and CFA (15 µm) compared to zeolites (5–9 µm). The only exception was 13X-Ag m.s. that presented the lowest diameter of particles (3 µm). It should be noted that the m.s. pellets had to be ground to powder, and the type and amount of binder should affect both the process of grinding as well as the particle size distribution of these fillers. The multimodal peaks observed (Fig. S1), in contrast to the single peak of zeolites size distribution, corroborate with this assumption. Following the zeolite pretreatments (washing and activation) it was observed a slight shift of granulometric distribution toward lower sizes. This behavior is illustrated for zeolite 4A, with decreases of average diameter from 4.8 ± 0.5 to 3.9 ± 0.1 µm after cleaning and calcination.

The zeolites are materials of high purity, in opposite to the other fillers that are m.s. which contain, in addition to the zeolite, binder materials. The EDX analyses put in evidence the heterogeneous chemical composition of m.s. with the presence of several elements besides zeolite framework components (Si, Al, O and Na as compensation cation). It was evidenced the presence of K and Ca in 3A m.s. and 5A m.s., respectively, and Ag in the 13X-Ag m.s., which was not surprising because it is containing about 35% Ag in its composition (according to supplier information). However, the presence of Fe, Mg, and Ti is not obvious and can be explained by the presence of binders, such as clays that may contain these elements in their framework. Several clays have been intensively used as fillers to improve PLA properties [47, 48], and it is possible to suppose that they may influence additionally the action of zeolites in PLA composites.

The identification and purity of zeolites were confirmed by XRD analysis (Suppl. Mat., Fig. S2). Unfortunately, it was not possible to identify the type of binders used on in the preparation of m.s. probably due to their low levels, below the sensitivity of the XRD technique. The most common binders used in molecular sieves (m.s.) processing are clays, selected from attapulgite, palygorskite, kaolin, sepiolite, bentonite, montmorillonite, and mixtures thereof. The clay content of the bonded m.s. can vary from as low as 1%, to as high as 40 wt%, although preferred range is 10–25% [49]. In the three tested m.s., the binder contents are more likely in the lower range.

We will concern also some aspects not enough considered up to now and which need better understanding where is considered the melt mixing of zeolites with a polyester (PLA) characterized by high water sensitivity. The presence of water, in its different forms, in zeolite framework could play an important role in PLA composite production, ulterior processing and in determining the properties of final products, such as the stability over time. Fillers water percentages were evaluated by TGA (Suppl. Mat., Fig. S3 (A, B)). It is observed that the water content (on wet basis) is increasing from 10.5% for Ag-exchanged m.s. up to 23.3% for 13X (Fig. S3B) with zeolite 4A presenting intermediary content (18.8%). In addition to the large variation in water content between the studied zeolites, the water molecules are linked to different sites in the zeolite structure through bonds more or less strong. This behavior is illustrated for zeolite 4A (Fig. S3A, DTG) with the maximum peak at 152 °C and a secondary peak at 345 °C corresponding to release of water molecules strongly bound on zeolite. The drying procedure (see experimental section) for removing the moisture from zeolite (105 °C for 2 h or until constant weight) must be used with caution. In these conditions, the drying does not completely remove the moisture

present in the zeolite, and a possible release of water molecules during production of PLA–zeolite composites may lead to the degradation of polymer matrix. In addition, some water could remain inside zeolite framework if the processing temperature is below the activation temperature of complete removal of water. This is the case of zeolite 4A which is only fully activated at ~450 °C, temperature well above those traditionally used in PLA composite processing (180–200 °C).

As reported in the literature, the role played by the water molecules present in the cavities and channels of zeolites appears to be of crucial importance. The presence of this "H_2O reservoir" and which can be released during the lifetime of the PLA composites, or in the course of processing as final products, could have possible undesirable impacts on PLA properties thereof. On the other hand, a water supply may be useful in post-consumer PLA degradation processes, increasing its recyclability.

Moreover, it is well known that zeolites, after dehydration by heating, may undergo a prompt rehydration [50]. Another aspect not taken into account in the processing of polymers with zeolites is the rapid absorption of water by activated zeolites. In most of the studies, zeolites are used without prior activation, and when activated, they are considered completely dehydrated, although is known their great ability to absorb humidity. In Fig. S4, the water vapor uptakes of activated 13X, Y, and 4A zeolites, calculated using the initial mass of the dry and activated sample (0% moisture), are shown. The water uptake is rapid and similar in the first hours for all zeolites, while the saturation has been observed after several hours. The final water content (on dry basis) for Y is 29%, which is respectively comparable or slightly bigger than those for 13X (28%) and 4A (25%). Additionally, in the insert of Fig. S4, the initial kinetics of water uptake after the first 5 min is shown and an average increase of 1.2% on zeolites weight was observed. This time was chosen as representative of the period in which the activated zeolite is in contact with ambient air before being mixing with the polymeric matrix by MB. Considering the addition into PLA of a zeolite loading of 5% and any loss of water during processing, the maximum moisture added to the composite/PLA will be above 600 parts per million (ppm). This value is much bigger than the one admitted for PLA (< 250 ppm moisture according to the supplier recommendation or even below 50 ppm in the case of PLA processed at high temperature [51]) to avoid the degradation provoked by the traces of water and to minimize the hydrolysis during melt processing. This result indicates that even in the case of activated zeolites, because of their quick rehydration, they could act as degradation agents in PLA–zeolite composites, and therefore, additional precautions should be taken when they are produced.

Evaluation of rheological parameters during melt blending

The significant influence of zeolites on the rheological behavior of polymer composites could already be observed during the melt-mixing process [52, 53]. In Fig. 1, the final torque and stock temperature (T_{stock}), measured in the end (after 7 min) processing, are presented. In the presence of a 5% zeolite, great part of fillers tested provokes a decrease in both the torque and T_{stock} compared with neat PLA (9.6 Nm,

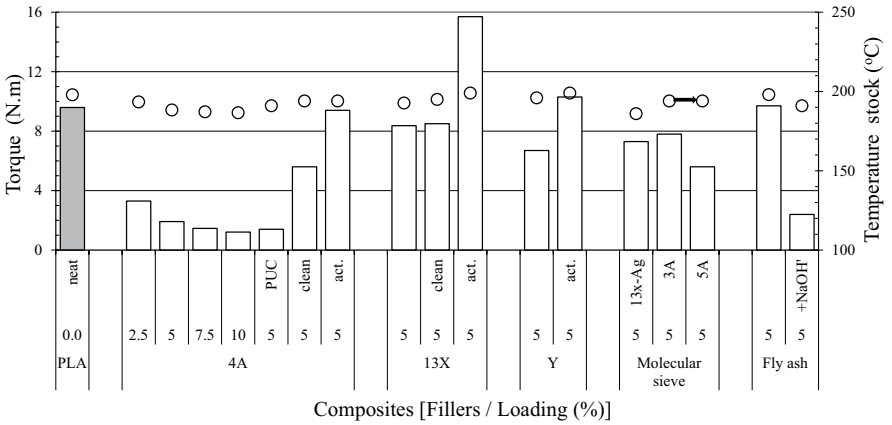

Fig. 1 Final torque and stock temperature measured in the end (7 min) of the melt-blending process of the neat PLA and PLA composites

198 °C). As the torque is directly determined by the viscosity of molten PLA blend, these results indicate probably the decrease in molecular weights during MB process following PLA degradation.

However, the effects are quite different: Whereas zeolite 13X induces a slight decrease in torque (8.4 Nm), zeolite 4A leads to dramatic decrease in this parameter (final torque of 1.9 Nm), while the m.s. and zeolite Y are presenting an intermediate influence (torque in the range 5.6–7.8 Nm). For T_{stock}, similar behavior was observed, with significant decreases (of about 10 °C) for PLA–4A composite compared with neat PLA. In Fig. 1 it is also possible to observe that the torque and T_{stock} are decreasing in quite good correlation (inversely correlated) with the loading of the zeolite 4A in PLA composites. However, these correlations are not linear, indicating the complexity of the phenomena involved.

The pretreatments of fillers (i.e., washing and activation) also influence the processing parameters of PLA with zeolites. Surprisingly, contrary to the untreated filler, a significant increase in both torque and T_{stock} was observed for the composite containing washed zeolite 4A (4A clean). Still higher values for torque (9.4 Nm) and T_{stock} (194 °C) were observed for the composite containing zeolite 4A previously activated (4A act.). Similar behavior was observed for activated zeolites 13X and Y. It should be noted the highest measured torque (15.7 N.m) was achieved for zeolite 13X act., a value 60% higher than those observed for neat PLA processed under similar conditions. Moreover, this result is well supported by the characterization of molecular parameters, which is reported in the next section.

As previously indicated in the literature [40, 41], coal fly ash (CFA) was tested because it presents a certain similarity with the zeolites and is raw material for the hydrothermal synthesis of zeolite $4A_{PUC}$. The presence of fly ash in the composite with PLA causes no change in torque and T_{stock}, at least 5% filler loading. However, when mixing with small amount (10:1 fly ash/alkali) of powder NaOH (< 250 µm, CFA_{NaOH}), the fly ash causes a strong decrease in both torque (2.4 Nm) and T_{stock}

(191 °C). The addition of alkali was considered because the zeolites are synthesized in strongly alkaline medium (usually NaOH), and even after intense washing, zeolite could keep a residual alkalinity. Some authors suggest the acceleration of PLA degradation in the presence of an alkaline medium [54]. These results are leading to the statement that the residual alkalinity of zeolites could participate, in a greater or lesser extent, to PLA degradation during melt-mixing process (details in the section Filler free alkalinity as source of PLA degradation).

These results suggest that zeolite 4A causes the most intense degradation of PLA among the fillers tested. Furthermore, based on these findings, different processing temperatures were tested (from 180 to 230 °C) to study the degradation of PLA composites containing this zeolite (i.e., 4A). The behaviors of the torque and T_{stock} are shown in Fig. 2. Filler loading in composites was 5%, except for the test at 230 °C, for which a smaller amount of zeolite 4A (1%) had to be used because of the full fluidization and advanced degradation of the blend at higher zeolite content. As expected, higher temperatures result in lower torque values, while the T_{stock} follow the profiles of processing temperature. However, the effect of zeolite on the decrease in torque and melt viscosity is clearly seen by comparing to the neat PLA.

Molar mass modification during PLA processing

It is worth recalling that the polyester-based matrix (i.e., PLA) is very sensitive during processing to the high temperature, shearing and hydrolysis, thus supplementary measures should be used to limit its degradation. The possible PLA degradation, or in some cases its depolymerization, due to the presence of zeolites, was also assessed by the analysis of molecular parameters. The evolution of M_n and dispersity (M_w/M_n) of neat PLA and PLA composites (at 5% filler loading) are shown in Fig. 3. Zeolite 4A without pretreatment presents a high degradation capacity (~90%

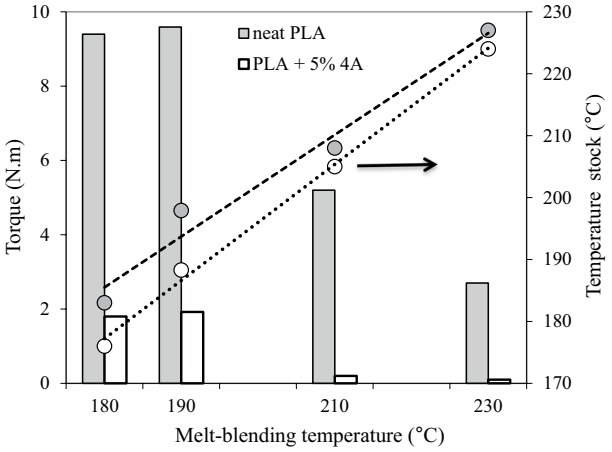

Fig. 2 Final torque and temperature measured in the end (7 min) of the melt-blending process of the neat PLA (gray color) and PLA–zeolite 4A composites (white color). The filler loading was 5%, except for test at 230 °C where a lower loading must be used (1%)

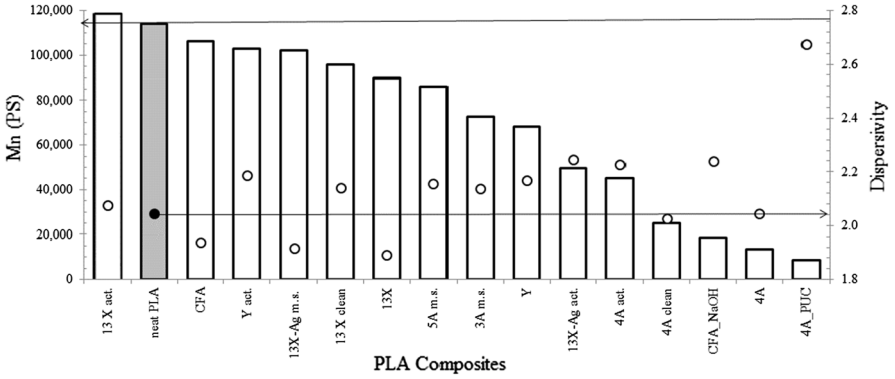

Fig. 3 Molar mass (M_n) and dispersity index (M_w/M_n) for neat PLA and PLA composites produced using 5% loading of different fillers. Lines used as guide to indicate the values for the neat PLA

decrease in M_n compared to the unfilled PLA processed in similar conditions), even in relative low loading (at 5% filler in composite). The washing process, used to decrease the free alkalinity of zeolites, and thermal activation partially decrease this capacity to 80% and 60%, respectively. This behavior is different for zeolite 13X that leads to a lower diminishing of PLA molecular weights (a reduction in M_n of only 18%). Furthermore, the previous zeolite cleaning decreases even more the degrading effect of this filler (i.e., decrease in M_n of only 13%). Moreover, somewhat surprising, the 13X act.(thermally activated zeolite) presents an unexpected behavior; the SEC data reveal a slight increase in PLA molar mass, an aspect that will be discussed in the next section. The dispersity index (Fig. 3) did not present a clear tendency, but the increases in filler loading (not shown here) seems to augment it, rather in good correlation with the level of PLA degradation. The m.s. tested presented intermediate degradation capacity. Finally, under the considered experimental conditions and using the MB approach, based on the molecular characterizations, the degrading effect of zeolites is decreasing as follows: $4A_{PUC} \approx 4A > CFA_{NaOH} > 4A$ clean $\gg 4A$ act. $> Y > 3A$ m.s. $> 5A$ m.s. $> 13X > 13X$ clean $> 13X$-Ag m.s. $> Y$ act $>$ CFA.

The degradation effect of zeolite 4A on PLA composites was also evaluated for different MB temperatures, as indicated in Table S2, which shows the M_n and dispersity of neat PLA and their counterparts processed at 190 °C (5% zeolite), 210 °C (5% zeolite), and 230 °C (1% zeolite). The smaller amount of zeolite 4A for the composite processed at 230 °C had to be used because processing problems, as previously explained. As expected, the increase in processing temperature causes a decrease in the M_n of both the neat PLA and composites. However, a more intense decrease in M_n for the composites (15% and 30%) than for the neat PLA (5% and 20%) is observed at higher processing temperatures (210 and 230 °C), reinforcing the important role of the filler in the degradation of the polymermatrix.

Furthermore, the influence of filler loading on PLA molar mass was studied for two zeolites (4A and 13X) and a molecular sieve (13X-Ag m.s.), and the results are shown in Fig. 4. These fillers were chosen as representative of the different behaviors previously observed. Moderate linear decreases in M_n correlated with filler

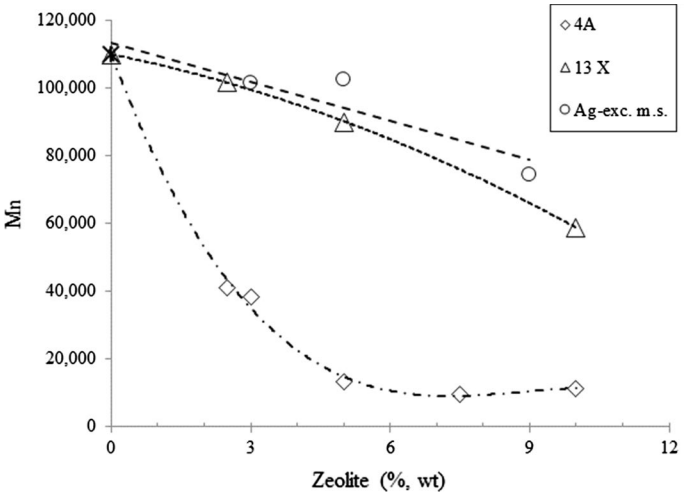

Fig. 4 Correlation between M_n of PLA composites and filler loading for zeolites 4A, 13X, and molecular sieve 13X-Ag m.s. Open symbols indicate filler used without pretreatment, while black and gray colors symbols indicated activated (act.) and washed (clean) zeolites, respectively

loading was observed for the composites containing zeolite 13X and molecular sieve 13X-Ag m.s. at higher tested loading (9–10%) the M_n decreases by 32–46%. The similar behavior for these fillers is probably due to their same zeolitic framework structure type (FAU—Faujasite). On the other hand, the molar mass of PLA from composites significantly falls in the presence of zeolite 4A. The greatest loss of M_n (about 92%) was initially observed for 5% loading. Supplementary additions of the zeolite 4A did not cause further M_n loss, at least for loading up to 10%.

Moreover, it is noteworthy mentioning that the influence of the overall processing (MB at 210 °C and subsequent hot pressing) on the modification of PLA molecular weights by degradation was studied at different residence time. PLA composites (with 5% zeolite 4A) were divided into two subsamples: One was subjected to standard compression molding procedure, while the other was not (indicated as "not pressed"). The evolutions of M_n of neat PLA and PLA–zeolite 4A composites after 3, 5, and 7 min of processing (i.e., MB at 210 °C) are shown in Fig. 5. The results indicated a significant decrease in M_n with the composite processing time. The subsequent compression molding has an important role being responsible for about 30% supplementary M_n decrease (total reduction about 89%) at the end of processing of the composite with the highest residence time (7 min), when compared to M_n of the neat PLA. These results suggest the strong degradation potential of zeolite 4A and the key role of the temperature as parameter, and thus the MB and ulterior processing should be evaluated carefully for the proper preparation of PLA–zeolite composites.

Finally, the results obtained using 4A allow to assume that this specific zeolite could be a product of interest in the chemical recycling of PLA by pyrolysis at high temperature (see the last section of this paper). They could represent an alternative to alkali earth metal oxides (CaO, MgO), ZnO, and other Zn compounds, e.g.,

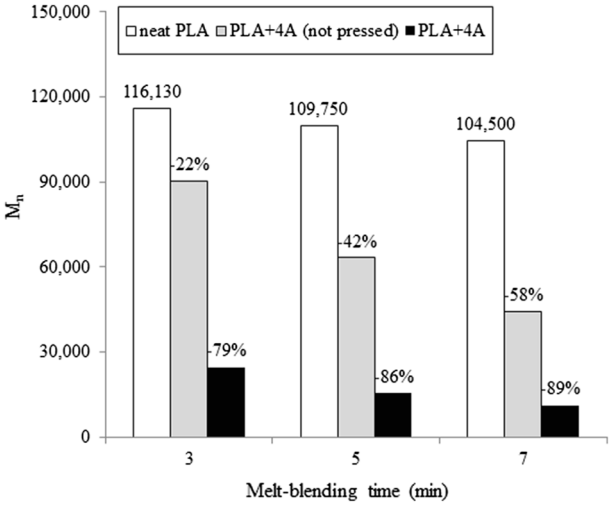

Fig. 5 Molar mass (M_n) profiles of neat PLA and PLA-4A composite (5% loading) in function of the time of the melt-blending process (210 °C). The not pressed indicated the composites samples that were not subjected to the compression molding procedure. The perceptual values indicate inside the figure, show the relative decrease in M_n of the composite compared to M_n of the neat PLA at same time interval

stannous 2-ethylhexanoate, etc., already known to catalyze the depolymerization of PLA [9, 55, 56].

Thermal properties of PLA–zeolite composites

Table 2 summarizes the results obtained following the thermal characterizations (DSC and TGA) of neat PLA and PLA–zeolite composites. The glass transition (T_g), cold crystallization (T_c) and melting (T_m) temperatures were not significantly affected by the m.s.13X-Ag and zeolites 13X and Y. On the other hand, the presence of zeolite 4A slightly decreases all temperatures, with more significant diminutions at high zeolite loading (i.e., 10 wt%). The decrease in T_c suggests that zeolite 4A may enhance the nucleation of PLA [33], but it is not excluded the influence of other factors, such as the formation of polymeric chains of lower molecular weights able to induce PLA crystallization at lower temperature. In addition, while neat PLA is nearly amorphous (degree of crystallinity about 3%), PLA–zeolite 4A composites show slightly higher percentages of crystallinity (8–10%). It is also noteworthy mentioning that the bimodal peaks of melting endotherms were recorded for great part of samples. As reported in other studies [32, 33, 43, 57], they can be attributed to several reasons, linked from crystal structures to processing conditions.

The thermal stability of PLA composites is greatly influenced by the nature of zeolites. Again, there are different behaviors among the tested fillers, with zeolite 4A causing the greatest decrease in the characteristic temperatures ($T_{5\%}$, $T_{50\%}$ and T_D). It is noteworthy that despite the worsening of stability, zeolite $4A_{PUC}$, synthetized using fly ash, presented a better thermal performance than its commercial

counterpart. Moreover, zeolite 13X induces a slight improvement in thermal performance of the respective composite. The other fillers had an intermediate behavior.

Regarding the influence of filler percentage, there is a decrease in the thermal stability of PLA–zeolite 4A composites with the increase in filler loading up to 7.5%. For higher amount (e.g., 10%), the characteristic temperatures keep the same level. Less significant variations were observed with the changing of the loading of zeolite 13X and m.s.13X-Ag. The washing and activation procedures of zeolite 4A improve significantly the thermal stability of composites. These results reinforce some data presented above. However, no clear trends were observed for the set of studied composites (Table 2).

Thus, for facility in the interpretation of data, a new approach is proposed based on the difference between the onset of thermal degradation ($T_{5\%}$) of the composites and neat PLA (ΔT). The degradation ratio, calculated by the division of the molar masses of composite and neat PLA, was plotted in function of this new parameter (Fig. 6). Composites with activated zeolites are above the trend line, having higher thermal stability when compared to their not-activated counterparts (see also Fig. S5). The zeolite 13X does not significantly change thermal stability of the composite causing only a marginal degradation. Even a small but measurable increase in M_n was observed for 13X act. filler (Fig. 8). The zeolite $4A_{PUC}$, produced from coal fly ash (CFA sample), causes a smaller decrease in thermal stability of the composite when compared to similar commercial zeolites 4A (decrease in $T_{5\%}$ by 50 °C and 80 °C, respectively). This result was not expected because $4A_{PUC}$ induced the highest decrease in M_n, among all tested fillers, which would suggest a greater decrease in thermal stability of its composite (Table 2).

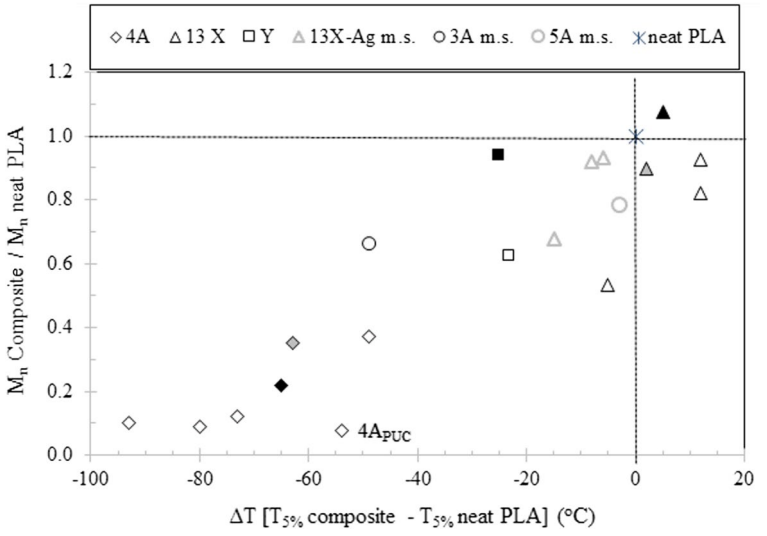

Fig. 6 Correlation of PLA degradation, estimated by the ratio M_n PLA composite/M_n neat PLA, and the difference between onset temperature (ΔT) taken as $T_{5\%loss}$ of PLA composite and neat PLA samples

Filler free alkalinity as source of PLA degradation

The previous results suggest that other additional factors than the structure and composition of the zeolite should intervene in the degradation of PLA composites. For instance, Yuzay and collaborators [33] observed the degradation of PLA in the presence of zeolite 4A, while somewhat surprisingly, natural zeolite (chabazite) is not degrading the polymer. These authors reported the production by MB of PLA–zeolite 4A composites (up to 5% filler) and realization of films characterized by good mechanical properties. However, these authors did not attempt to explain the reasons for this remarkable difference in the behavior of these zeolites, so similar in many ways.

As shown in the introductive part, there are several reports regarding the degradation of polymers (PP, PE, PET, etc.) induced by zeolites as residual catalysts or added as filler. In many cases, the degradation is explained in function of the acid sites and presents on the zeolites surface and inside of their framework. Correlations between the intensity of degradation and zeolite types have been suggested to explain this complex issue. In most of the cases, the different acidities among zeolites are pointed out as the major factor for polymer degradation. However, the acid sites are located inside the cage of zeolites, which hinders the access of large molecules such as PLA. It is reasonable to assume that if depolymerization occurs only in these acid sites, the process would be slow and would not lead to a significant decrease in M_n. This is not the case for some tested fillers tested, and especially for zeolite 4A. This suggests that other factors must be taken into account, among them, the residual alkalinity should be also considered.

One aspect less studied is the presence of alkalinity on zeolites surface, following the synthesis, which is mediated by concentrated alkali and not completely eliminated by washing processes. Thus, this parameter needs further consideration in the perspective of MB with PLA. A simple analysis to evaluate the "free" alkalinity effect of the zeolites was performed, following a standard test used in industry (kindly suggested by IQE, Spain). In Fig. 7, the correlation between free alkalinity of zeolites and degradation ratio, estimated by the decreasing of M_n of the composite compared to M_n of the neat PLA, is presented. The data used correspond to a zeolite loading of 5% (4A and 13X) and 6% (13X-Ag m.s.). Two distinct behaviors have been seen (Fig. 7 Frames I and II), the most advanced degradation corresponding to zeolites characterized by high free alkalinity (zeolite 4A products, Frame I). The decrease in PLA molecular weights by zeolites was found as following this order: I ($4A_{PUC} \approx 4A > 4A$ act $> 4A$ clean) $\gg$ II (Y > 3A m.s. > 5A m.s. > 13X > 13X clean. > Ag-exc. m.s. > 13X act). Accordingly, the level of "free alkalinity" could be a significant parameter that can explain the degradation of PLA, as clearly evidenced in the case of zeolites 4A having different treatments.

Furthermore, connected to the recycling of PLA wastes, it is important to precise that on the one hand, the alcoholic solutions of both, alkali metal hydroxides and alkali metal carbonates, were found to be able to depolymerize PLA and to provide high quality lactic acid monomers in high yield [58]. On the other hand, most people agree that the degradation of PLA and its oligomers is faster in solutions with elevated pH, while the presence of terminal hydroxy groups was found to accelerate

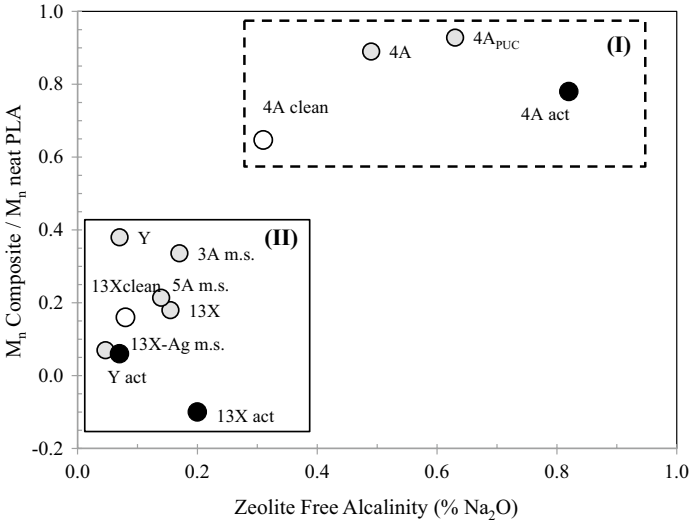

Fig. 7 Correlation between degradation ratio (M_n PLA composite/M_n neat PLA) and free alkalinity of zeolites (4A, 13X, and Y) and molecular sieves (3A m.s., 5A m.s.,13X-Ag m.s.) at 5% fillers loading. The open, black and gray circles indicate washed (clean), activated (act.), and untreated fillers, respectively

this process [59]. The suggested degradation mechanism (Fig. 8) is ascribed to the intramolecular backbiting reaction from hydroxyl chain end leading to the formation of lactide and oligomers of lower molecular weights.

Gaseous products evolved under dynamic heating during the thermal degradation of PLA–zeolite composites

Figure 9 shows the traditional mechanism ascribed to the degradation of PLA by pyrolysis. It has been reported that the PLA thermal degradation is a complex phenomenon which predominantly consists of random main-chain scission and

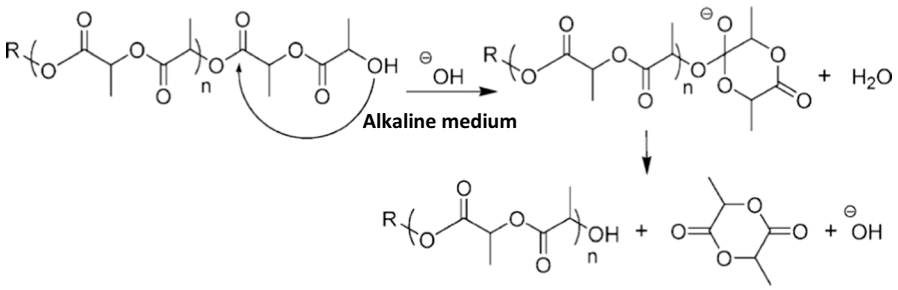

Fig. 8 Suggested mechanism to illustrate the degradation by backbiting of PLA and its oligomers in alkaline medium to form lactide. Adapted with permission from: Xu L, Crawford K, Gorman CB (2011) [54]. Copyright (2011) American Chemical Society

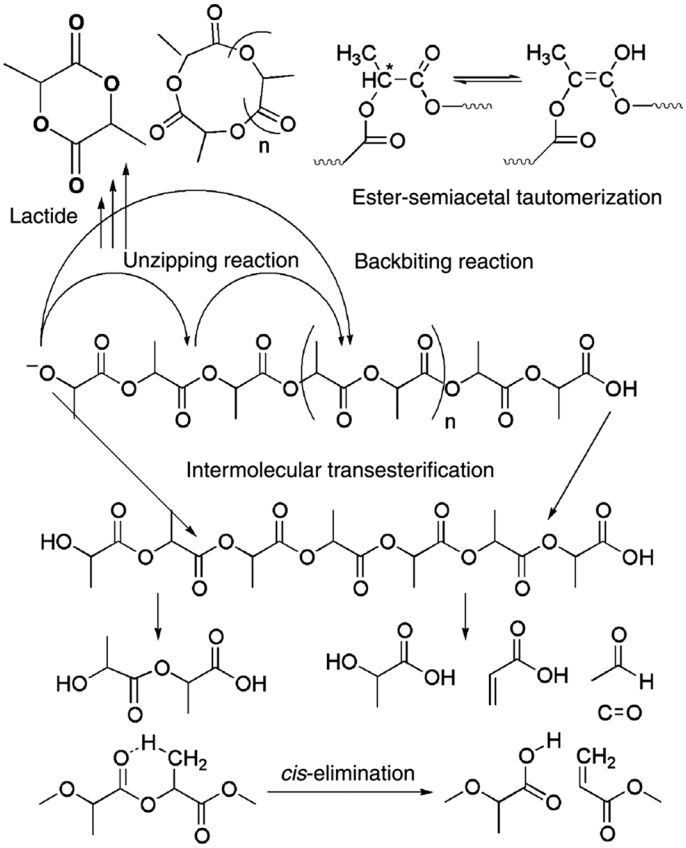

Fig. 9 Thermal degradation of PLA and pyrolysis mechanism. Reprinted from Ref. [60]

unzipping depolymerization reactions [60, 61]. The random degradation involves intramolecular and intermolecular transesterifications, cis-elimination, other reactions, such as of hydrolysis or oxidative degradation. Besides, it is agreed that the dominant reactions of thermal degradation are the intramolecular and intermolecular transesterifications leading to cyclic oligomers of lactic acid and lactide [62, 63]. Unzipping depolymerization (backbiting degradation) is evidenced when terminal hydroxyl groups became more concentrated [64].

The hydrolytic degradation must be also considerate as a competitive reaction depending on the water content, and certainly plays an important role in the PLA–zeolite composites. The high hydrophilic character of zeolites tested in this study and their rapid rehydratation indicate the presence of water on composite at not negligible levels. The observed strong influence of residual alkalinity of the zeolite on PLA thermal degradation suggests the important role of solid base in this process. Similar behavior was observed in the thermal degradation of polystyrene using solid bases that have been more effective catalysts than solid acids, such as zeolite HSM-5 [65]. It is noteworthy also to mention that almost all PLA active

chain end groups, residual monomer, and polymerization catalysts (e.g., Sn derivatives), residual metals such those from zeolites (Ca, Mg, Al, etc.) are known to accelerate the thermal degradation of PLA [66, 67].

The complex PLA thermal degradation mechanism generates, besides oligomers of lactic acid and lactide, other degradation products such as CO, CO_2, acetaldehyde, and methyl ketone [62, 68]. The presence of these degradation byproducts was confirmed for both PLA and PLA composites.

In this study, the PLA composite thermal degradation was evaluated by TGA coupled to a FTIR detector that permitted the determination of the volatile sub-products generated. The 3D TG-FTIR spectra obtained at heating rate of 10 °C min^{-1} are presented in Fig. 10 and Fig S6 (Suppl. Mat.). For all samples tested, it is observed the greatest volatile compounds release in the range of 2000–2400 s that correspond to the interval of temperatures 275–390 °C. After that time, a gradual decrease in absorption bands is observed.

Figure 10 shows the comparative FTIR spectra obtained during TGA of both, neat PLA (Fig. 10a, c) and PLA–zeolite 4A composites (Fig. 10b, d), produced by MB at 190 °C and 230 °C. All samples have the same absorption bands but with different intensities. More specifically, zeolite 4A is found to significantly

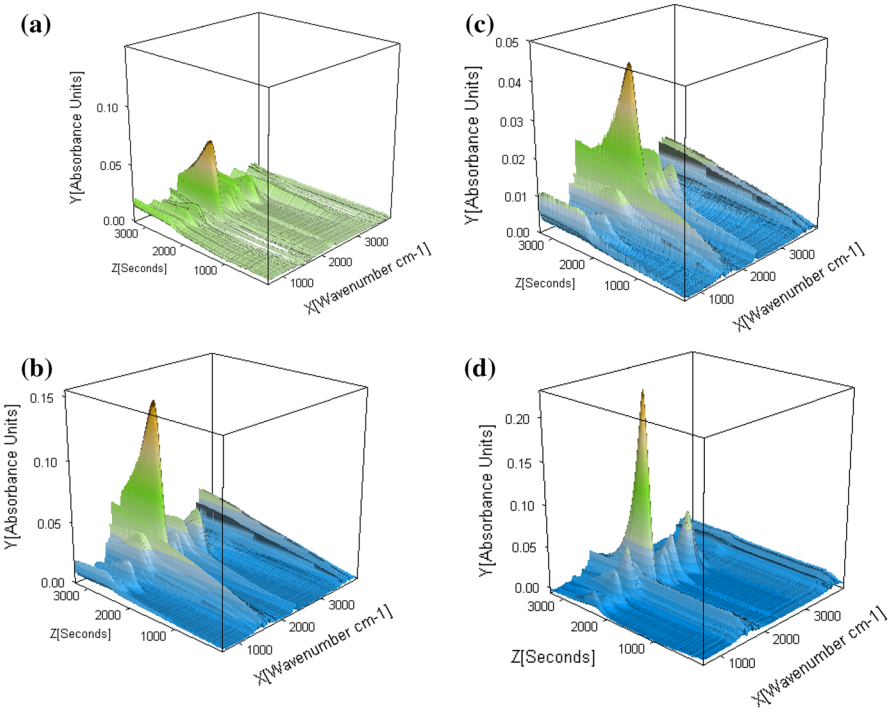

Fig. 10 3D-FTIR spectra of the evolved gaseous products (N_2 flow 10 °C min^{-1}) of **a** neat PLA and **b** PLA–5% zeolite 4A composite processed at T_{MB} of 190 °C; **c** neat PLA and **d** PLA–1% zeolite 4A processed at T_{MB} of 230 °C

promote the generation of volatile compounds. For example, the most intense band (1761 cm^{-1}) increased 2.5 and 4.4 times in the composites produced at 190 °C and 230 °C, respectively, when compared to the neat PLA. These results are expected by considering the dramatic decrease observed in M_n of composites compared to the neat PLA prepared at similar temperatures (Table S2).

The FTIR spectrum obtained at the maximum evolution gas products rate (365 °C) during the thermal degradation of PLA–1% zeolite 4A composite (processed at 230 °C) are shown in Fig. 11a. This composite was chosen because present the most intense degradation (Table S2). The most intense peak at 1761 cm^{-1} is attributed to aldehyde group that also present characteristic peaks at 2730 cm^{-1}, corresponding to the C=O band stretching vibration and the aldehydic C–H stretching vibration, respectively [10, 57, 68–71]. Other characteristics peaks of CO_2 (2355 cm^{-1} and 2318 cm^{-1}), CO (2168 cm^{-1} and 2098 cm^{-1}), and aliphatic esters (1761 cm^{-1} and 1111 cm^{-1}) are also present in different intensities.

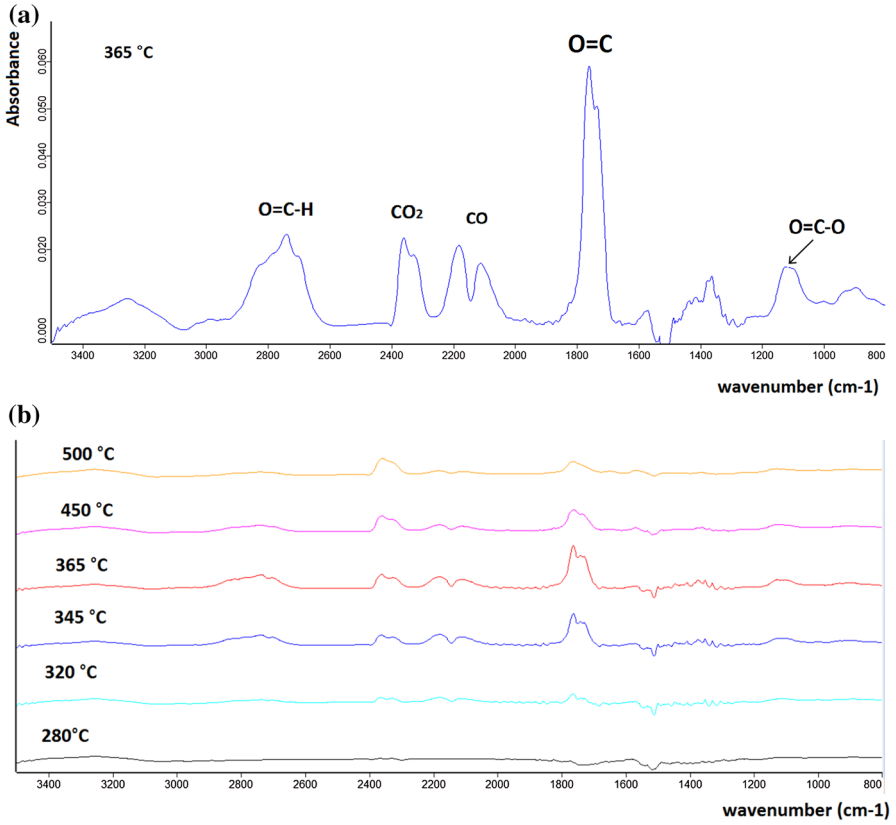

Fig. 11 FTIR spectra of gaseous products evolved by TGA analysis at **a** 365 °C and **b** in the temperature range 280–500 °C for PLA–4A composite (1%, T_{MB} 230 °C) using N_2 flow and a heating rate of 10 °C min^{-1}

For a better understanding of the process regarding the formation of these products, the spectra of gas products at different temperatures (280 °C up to 500 °C) are plotted in Fig. 11b. The carbonyl compounds are the main products obtained following PLA–zeolite composite thermal degradation and their trends are like that of CO and of species containing aliphatic esters. The presence of these compounds can be clearly observed from 320 °C with an increase up to 365 °C, and after, a similar decline for higher temperatures. At the beginning of the pyrolysis, the CO_2 follows the same trend, but the intensity of characteristic peaks continues to accentuate with the increase in temperature. At the maximum evaluated temperature (500 °C), CO_2 becomes the main product of degradation, which is attributed to the PLA chain homolysis [70–72].

In Fig. S6 (Suppl. Mat.), the FTIR spectra of gaseous products evolved by PLA composites filled with different zeolites (13X, 4A and Y) are also shown. For instance, similar profiles were observed indicating that the same volatile sub-products are generated by the three composites despite the very different behaviors previously discussed.

Finally, it is assumed that an isothermal heating program and even lower temperatures of testing than those of T_D (e.g., 250–300 °C) in association with other techniques of analysis (e.g., pyrolysis–gas chromatograph/mass spectra—Py-GC/MS) can lead to more specific results compared with the dynamic heating using TGA.

Conclusions

In this work, a screening of different types of zeolites and molecular sieves, containing zeolites, as well as a coal fly ash, was performed with the objective to evaluate their influence on PLA catalytic depolymerization during composites preparation and processing. In addition, the thermal stability of the resulting composites was also studied in the perspective of elaboration of PLA composites with recycling ability through a catalytic depolymerization process.

More specifically, several amounts of zeolites exhibiting different chemical compositions (4A, Y, 3A m.s., 5A m.s., 13X, 13X Ag m.s. and CFA) and various size distributions were tested with a PLA matrix under different processing conditions and the evaluation of the molecular, rheological, and thermal parameters of the elaborated PLA composites was performed.

The results of this work show that the PLA molar mass reduction upon processing and the state of thermal degradation induced by zeolite fillers is mainly related to the nature of the zeolite. More specifically, increased degradation of PLA was observed in the following order: 4A $\gg$ Y > 3A m.s. > 5A m.s. > 13X > 13X Ag m.s. > CFA.

Interestingly, the washing and pretreatments of zeolites were found to diminish in some cases their degradation capacity during their processing with PLA. The decrease in free alkalinity may explain the effect of the washing for polymer stability, especially in the case of zeolite 4A for which the activation appears to induce a more complex change in the zeolite reactivity toward PLA. The results of the study suggest that the stronger degradation potential is achieved for untreated zeolite 4A

which seems a product of interest for the chemical recycling of PLA by pyrolysis at high temperature.

Acknowledgements The authors from the University of Mons & Materia Nova thank the Wallonia Region, Nord-Pas de Calais Region and European Community for the financial support in the frame of the INTERREG IV—NANOLAC project and FEDER 2014-2020 program (PROSTEM project). M. Pires thank to the University of Mons, PUCRS and CNPq (Grants 309623/2012-0; 551433/2010-8) for the post-doc grant and financial support. A. Cardoso thanks CAPES for Ph.D. Grant (01714947092). Special thanks are addressed to Mr. Francisco CACHO (IQE, Spain) for zeolite samples and their characterization, information kindly sent for utilization in the frame of this study. The authors thank to Dr. Olivier Persenaire, Anne-Laure Dechief and OlteaMurariu from Materia Nova R&D Center for helpfully discussions and assistance in the preparation and characterization of samples.

References

1. Auras R, Harte B, Selke S (2004) An overview of polylactides as packaging materials. Macromol Biosci 4:835–864. https://doi.org/10.1002/mabi.200400043
2. Jamshidian M, Tehrany EA, Imran M et al (2010) Poly-lactic acid: production, applications, nanocomposites, and release studies. Compr Rev Food Sci Food Saf 9:552–571. https://doi.org/10.1111/j.1541-4337.2010.00126.x
3. Madhavan NK, Nair NR, John RP (2010) An overview of the recent developments in polylactide (PLA) research. Bioresour Technol 101:8493–8501. https://doi.org/10.1016/j.biortech.2010.05.092
4. Perego G, Cella GD (2010) Mechanical Properties. Poly(Lactic Acid). Wiley, New York, pp 141–153
5. Raquez J-M, Habibi Y, Murariu M, Dubois P (2013) Polylactide (PLA)-based nanocomposites. Prog Polym Sci 38:1504–1542. https://doi.org/10.1016/j.progpolymsci.2013.05.014
6. Anderson KS, Schreck KM, Hillmyer MA (2008) Toughening polylactide. Polym Rev 48:85–108. https://doi.org/10.1080/15583720701834216
7. Murariu M, Bonnaud L, Yoann P et al (2010) New trends in polylactide (PLA)-based materials: "Green" PLA–Calcium sulfate (nano)composites tailored with flame retardant properties. Polym Degrad Stab 95:374–381. https://doi.org/10.1016/j.polymdegradstab.2009.11.032
8. Rasal RM, Janorkar AV, Hirt DE (2010) Poly(lactic acid) modifications. Prog Polym Sci 35:338–356. https://doi.org/10.1016/j.progpolymsci.2009.12.003
9. Abe H, Takahashi N, Kim KJ et al (2004) Thermal degradation processes of end-capped poly(L-lactide)s in the presence and absence of residual zinc catalyst. Biomacromol 5:1606–1614. https://doi.org/10.1021/bm0497872
10. Patwa R, Singh M, Kumar A, Katiyar V (2018) Kinetic modelling of thermal degradation and non-isothermal crystallization of silk nano-discs reinforced poly (lactic acid) bionanocomposites. Polym Bull 76:1349–1382. https://doi.org/10.1007/s00289-018-2434-7
11. Gu L, Qiu J, Qiu C et al (2018) Mechanical properties and degrading behaviors of aluminum hypophosphite-poly(Lactic Acid) (PLA) nanocomposites. Polym Plast Technol Eng 58(2):126–138. https://doi.org/10.1080/03602559.2018.1466169
12. Okamoto K, Toshima K, Matsumura S (2005) Degradation of poly(lactic acid) into repolymerizable oligomer using montmorillonite K10 for chemical recycling. Macromol Biosci 5:813–820. https://doi.org/10.1002/mabi.200500086
13. Panda AK, Singh RK, Mishra DK (2010) Thermolysis of waste plastics to liquid fuel: a suitable method for plastic waste management and manufacture of value added products—A world prospective. Renew Sustain Energy Rev 14:233–248. https://doi.org/10.1016/j.rser.2009.07.005
14. Al-Salem SM, Lettieri P, Baeyens J (2009) Recycling and recovery routes of plastic solid waste (PSW): a review. Waste Manag 29:2625–2643. https://doi.org/10.1016/j.wasman.2009.06.004
15. Al-Salem SM, Lettieri P, Baeyens J (2010) The valorization of plastic solid waste (PSW) by primary to quaternary routes: from re-use to energy and chemicals. Prog Energy Combust Sci 36:103–129. https://doi.org/10.1016/j.pecs.2009.09.001
16. Cleetus C, Thomas S, Varghese S (2013) Synthesis of petroleum-based fuel from waste plastics and performance analysis in a CI engine. J Energy 2013:10. https://doi.org/10.1155/2013/608797

17. Dickerson T, Soria J (2013) Catalytic fast pyrolysis: a review. Energies 6:514. https://doi.org/10.3390/en6010514
18. Huang Z, Guo Y, Zhang T et al (2013) Fabrication and characterizations of zeolite β–filled polyethylene composite films. Packag Technol Sci 26:1–10. https://doi.org/10.1002/pts.1986
19. Feng C, Zhang Y, Liu S et al (2013) Synergistic effects of 4A zeolite on the flame retardant properties and thermal stability of a novel halogen-free PP/IFR composite. Polym Adv Technol 24:478–486. https://doi.org/10.1002/pat.3108
20. Kim H-S, Kim H-J (2008) Influence of the zeolite type on the mechanical–thermal properties and volatile organic compound emissions of natural-flour-filled polypropylene hybrid composites. J Appl Polym Sci 110:3247–3255. https://doi.org/10.1002/app.28853
21. Fernández A, Soriano E, Hernández-Muñoz P, Gavara R (2010) Migration of antimicrobial silver from composites of polylactide with silver zeolites. J Food Sci 75:E186–E193. https://doi.org/10.1111/j.1750-3841.2010.01549.x
22. Baerlocher C, McCusker LB, Olson DH (2007) Atlas of zeolite framework types, 6th revised edn. Elsevier, Amsterdam
23. Kim H-S, Lee B-H, Kim H-J, Yang H-SS (2011) Mechanical-thermal properties and VOC emissions of natural-flour-filled biodegradable polymer hybrid bio-composites. J Polym Environ 19:628–636. https://doi.org/10.1007/s10924-011-0313-5
24. Jiraroj D, Tungasmita S, Tungasmita DN (2014) Silver ions and silver nanoparticles in zeolite A composites for antibacterial activity. Powder Technol 264:418–422. https://doi.org/10.1016/j.powtec.2014.05.049
25. Fonseca AM, Neves IC (2013) Study of silver species stabilized in different microporous zeolites. Microporous Mesoporous Mater 181:83–87. https://doi.org/10.1016/j.micromeso.2013.07.018
26. Audisio G, Bertini F, Beltrame PL, Carniti P (1992) Catalytic degradation of polyolefins. Makromol Chemie Macromol Symp 57:191–209. https://doi.org/10.1002/masy.19920570117
27. Neves IC, Botelho G, Machado AV, Rebelo P (2006) The effect of acidity behaviour of Y zeolites on the catalytic degradation of polyethylene. Eur Polym J 42:1541–1547. https://doi.org/10.1016/j.eurpolymj.2006.01.021
28. Coelho A, Costa L, Marques MM et al (2012) The effect of ZSM-5 zeolite acidity on the catalytic degradation of high-density polyethylene using simultaneous DSC/TG analysis. Appl Catal A Gen 413:183–191. https://doi.org/10.1016/j.apcata.2011.11.010
29. Durmuş A, Koç SN, Pozan GS et al (2005) Thermal-catalytic degradation kinetics of polypropylene over BEA, ZSM-5 and MOR zeolites. Appl Catal B Environ 61:316–322. https://doi.org/10.1016/j.apcatb.2005.06.009
30. Gobin K, Manos G (2004) Thermogravimetric study of polymer catalytic degradation over microporous materials. Polym Degrad Stab 86:225–231. https://doi.org/10.1016/j.polymdegradstab.2004.05.001
31. Auras R, Selke S, Yuzay IE (2010) Poly(Lactic Acid) and zeolite composites and method of manufacturing the same, Patent US20100236969A1
32. Yuzay IE, Auras R, Selke S (2010) Poly(lactic acid) and zeolite composites prepared by melt processing: morphological and physical–mechanical properties. J Appl Polym Sci 115:2262–2270. https://doi.org/10.1002/app.31322
33. Yuzay IE, Auras R, Soto-Valdez H, Selke S (2010) Effects of synthetic and natural zeolites on morphology and thermal degradation of poly(lactic acid) composites. Polym Degrad Stab 95:1769–1777. https://doi.org/10.1016/j.polymdegradstab.2010.05.011
34. Ye Q, Huang Z, Hao Y et al (2016) Kinetic study of thermal degradation of poly(l-lactide) filled with β-zeolite. J Therm Anal Calorim 124:1471–1484. https://doi.org/10.1007/s10973-016-5314-0
35. Bendahou D, Bendahou A, Grohens Y, Kaddami H (2015) New nanocomposite design from zeolite and poly(lactic acid). Ind Crops Prod 72:107–118. https://doi.org/10.1016/j.indcrop.2014.12.055
36. Pires M, Murariu M, Cardoso MA et al (2013) Synthesis and characterization of novel zeolite poly(lactic acid) composites. In: Proceedings of the 12th Brazilian congress on polymers, Florianópolis, Brazil
37. Hao YH, Huang Z, Wang JW et al (2016) Improved thermal stability of poly (l-lactide) with the incorporation of zeolite ZSM-5. Polym Test 49:46–56. https://doi.org/10.1016/j.polymertesting.2015.11.010
38. Hao Y, Huang Z (2018) Effects of different zeolites on poly(L-Lactide) thermal degradation BT. In: Ouyang Y, Xu M, Zhao P et al (eds) Applied sciences in graphic communication and packaging. Springer, Singapore, pp 849–855

39. Gregorova A, Machovsky M, Wimmer R (2012) Viscoelastic properties of mineral-filled poly(lactic acid) composites. Int J Polym Sci 2012:1–6. https://doi.org/10.1155/2012/252981
40. Cardoso AM, Horn MB, Ferret LS et al (2015) Integrated synthesis of zeolites 4A and Na-P1 using coal fly ash for application in the formulation of detergents and swine wastewater treatment. J Hazard Mater 287:69. https://doi.org/10.1016/j.jhazmat.2015.01.042
41. Cardoso AM, Paprocki A, Ferret LS et al (2015) Synthesis of zeolite Na-P1 under mild conditions using Brazilian coal fly ash and its application in wastewater treatment. Fuel 139:59–67. https://doi.org/10.1016/j.fuel.2014.08.016
42. Fischer EW, Sterzel HJ, Wegner G (1973) Investigation of the structure of solution grown crystals of lactide copolymers by means of chemical reactions. Kolloid-Zeitschrift Zeitschrift für Polym 251:980–990. https://doi.org/10.1007/BF01498927
43. Murariu M, Doumbia A, Bonnaud L et al (2011) High-performance polylactide/ZnO nanocomposites designed for films and fibers with special end-use properties. Biomacromolecules 12:1762–1771. https://doi.org/10.1021/bm2001445
44. Kutchko BG, Kim AG (2006) Fly ash characterization by SEM-EDS. Fuel 85:2537–2544. https://doi.org/10.1016/j.fuel.2006.05.016
45. Ferrarini SF, Cardoso AM, Paprocki A, Pires M (2016) Integrated synthesis of zeolites using coal fly ash: element distribution in the products, washing waters and effluent. J Braz Chem Soc 27:2034–2045. https://doi.org/10.5935/0103-5053.20160093
46. Melo CR, Riella HG, Kuhnen NC et al (2012) Synthesis of 4A zeolites from kaolin for obtaining 5A zeolites through ionic exchange for adsorption of arsenic. Mater Sci Eng B 177:345–349. https://doi.org/10.1016/j.mseb.2012.01.015
47. Okamoto M (2012) Polylactide/clay nano-biocomposites. In: Avérous L, Pollet E (eds) Environmental silicate nano-biocomposites. Springer, London, pp 77–118
48. Sinha Ray S, Okamoto M, Ray SS et al (2003) Biodegradable polylactide and its nanocomposites: opening a new dimension for plastics and composites. Macromol Rapid Commun 24:815–840. https://doi.org/10.1002/marc.200300008
49. Breck DW (1978) Zeolite molecular sieves. Wiley-Interscience, New York
50. Esposito S, Marocco A, Dell'Agli G et al (2015) Relationships between the water content of zeolites and their cation population. Microporous Mesoporous Mater 202:36–43. https://doi.org/10.1016/j.micromeso.2014.09.041
51. Lim L-TT, Auras R, Rubino M (2008) Processing technologies for poly(lactic acid). Prog Polym Sci 33:820–852. https://doi.org/10.1016/j.progpolymsci.2008.05.004
52. Filippone G, Carroccio SC, Curcuruto G et al (2015) Time-resolved rheology as a tool to monitor the progress of polymer degradation in the melt state e Part II: thermal and thermo-oxidative degradation of polyamide 11/organo-clay nanocomposites. Polymer (Guildf) 73:102–110
53. Filippone G, Carroccio SC, Mendichi R et al (2015) Time-resolved rheology as a tool to monitor the progress of polymer degradation in the melt state—Part I: thermal and thermo-oxidative degradation of polyamide 11. Polymer (Guildf) 72:134–141. https://doi.org/10.1016/j.polymer.2015.06.059
54. Carrasco F, Pags P, Gámez-Pérez J et al (2010) Kinetics of the thermal decomposition of processed poly(lactic acid). Polym Degrad Stab 95:2508–2514. https://doi.org/10.1016/j.polymdegradstab.2010.07.039
55. Fan Y, Nishida H, Mori T et al (2004) Thermal degradation of poly(l-lactide): effect of alkali earth metal oxides for selective l, l-lactide formation. Polymer (Guildf) 45:1197–1205. https://doi.org/10.1016/j.polymer.2003.12.058
56. Narayan R, Wu WM, Criddle CS et al (2013) Lactide production from thermal depolymerization of PLA with applications to production of PLA or other bioproducts. 1 United States Patent Application 20130023674
57. Pluta M (2004) Morphology and properties of polylactide modified by thermal treatment, filling with layered silicates and plasticization. Polymer (Guildf) 45:8239–8251. https://doi.org/10.1016/j.polymer.2004.09.057
58. Srinivasan G, Grewell D (2013) Depolymerization of polylactic acid, Patent US20130096342A1
59. Xu L, Crawford K, Gorman CB (2011) Effects of temperature and pH on the degradation of poly(lactic acid) brushes. Macromolecules 44:4777–4782. https://doi.org/10.1021/ma2000948
60. Nishida H (2010) Thermal Degradation. In: Auras R, Lim LT, Selke S, Tsuji H (eds) Poly(Lactic Acid). Wiley, New York, pp 401–412

61. Abe H, Takahashi N, Kim KJ, Mochizuki M (2004) Thermal degradation processes of end-capped poly(L-lactide) s in the presence and absence of residual zinc catalyst. Biomacromolecules 5:1606–1614
62. Kopinke FD, Remmler M, Mackenzie K et al (1996) Thermal decomposition of biodegradable polyesters—II. Poly(lactic acid). Polym Degrad Stab 53:329–342. https://doi.org/10.1016/0141-3910(96)00102-4
63. Wachsen O, Reichert KH, Krüger RP et al (1997) Thermal decomposition of biodegradable polyesters—III. Studies on the mechanisms of thermal degradation of oligo-L-lactide using SEC, LACCC and MALDI-TOF-MS. Polym Degrad Stab 55:225–231. https://doi.org/10.1016/S0141-3910(96)00127-9
64. Liu X, Zou Y, Li W et al (2006) Kinetics of thermo-oxidative and thermal degradation of poly(d, l-lactide) (PDLLA) at processing temperature. Polym Degrad Stab 91:3259–3265. https://doi.org/10.1016/j.polymdegradstab.2006.07.004
65. Ukei H, Hirose T, Horikawa S et al (2000) Catalytic degradation of polystyrene into styrene and a design of recyclable polystyrene with dispersed catalysts. Catal Today 62:67. https://doi.org/10.1016/S0920-5861(00)00409-0
66. Feng L, Feng S, Bian X et al (2018) Pyrolysis mechanism of Poly(lactic acid) for giving lactide under the catalysis of tin. Polym Degrad Stab 157:212–223. https://doi.org/10.1016/j.polymdegradstab.2018.10.008
67. Castro-Aguirre E, Iñiguez-Franco F, Samsudin H et al (2016) Poly(lactic acid)—mass production, processing, industrial applications, and end of life. Adv Drug Deliv, Rev
68. Zou H, Yi C, Wang L et al (2009) Thermal degradation of poly(lactic acid) measured by thermogravimetry coupled to Fourier transform infrared spectroscopy. J Therm Anal Calorim 97:929–935. https://doi.org/10.1007/s10973-009-0121-5
69. Chen X, Zhuo J, Jiao C (2012) Thermal degradation characteristics of flame retardant polylactide using TG-IR. Polym Degrad Stab 97:2143–2147. https://doi.org/10.1016/j.polymdegradstab.2012.08.016
70. Herrera-Kao WA, Loría-Bastarrachea MI, Pérez-Padilla Y et al (2018) Thermal degradation of poly(caprolactone), poly(lactic acid), and poly(hydroxybutyrate) studied by TGA/FTIR and other analytical techniques. Polym Bull 75:4191–4205. https://doi.org/10.1007/s00289-017-2260-3
71. McNeill IC, Leiper HA (1985) Degradation studies of some polyesters and polycarbonates-1. Polylactide: general features of the degradation under programmed heating conditions. Polym Degrad Stab 11:267–285. https://doi.org/10.1016/0141-3910(85)90050-3
72. He DL, Yin GF, Dong FQ et al (2010) Research on the additives to reduce radioactive pollutants in the building materials containing fly ash. J Hazard Mater 177:573–581. https://doi.org/10.1016/j.jhazmat.2009.12.071